

Semi-automatically quantified tumor volume using Ga-68-PSMA-11-PET as biomarker for survival in patients with advanced prostate cancer

Robert Seifert^{1,2,3,4}, Ken Herrmann^{2,3,4}, Jens Kleesiek^{3,5}, Michael Schäfers^{1,4}, Vijay
Shah⁶, Zhoubing Xu⁷, Guillaume Chabin⁷, Sasa Grbic⁷,
Bruce Spottiswoode⁶ and Kambiz Rahbar^{1,4}

1. Department of Nuclear Medicine, University Hospital Münster, Münster, Germany
2. Department of Nuclear Medicine, University Hospital Essen, Essen, Germany
3. German Cancer Consortium (DKTK)
4. West German Cancer Center
5. Division of Radiology, German Cancer Research Center, Heidelberg, Germany
6. Siemens Medical Solutions USA, Inc., Knoxville, TN, United States
7. Siemens Medical Solutions USA, Inc., Princeton, NJ, United States

Short title: PSMA-PET-CT tumor volume in prostate cancer

Key words: PSMA-PET-CT; Prostate cancer; image biomarker; tumor volume

Word count: 5242 (total)

Corresponding Author:

Kambiz Rahbar MD

Department of Nuclear Medicine

University Hospital Münster

Albert-Schweitzer-Campus 1

D-48149 Münster

Germany

Tel: +49-251-8347362

Fax: +49-251-8347363

rahbar@uni-muenster.de

Abstract

Introduction

Prostate specific membrane antigen (PSMA) targeting Positron Emission Tomography (PET) imaging is becoming the reference standard for prostate cancer (PC) staging, especially in advanced disease. Yet, the implications of PSMA-PET derived whole-body tumor volume for overall survival are poorly elucidated to date. This might be due to the fact that (semi-) automated quantification of whole-body tumor volume as PSMA-PET biomarker is an unmet clinical challenge. Therefore, a novel semi-automated software is proposed and evaluated by the present study, which enables the semi-automated quantification of PSMA-PET biomarkers such as whole-body tumor volume.

Methods

The proposed quantification is implemented as a research prototype (MI Whole Body Analysis Suite, v1.0, Siemens Medical Solutions USA, Inc., Knoxville, TN). PSMA accumulating foci were automatically segmented by a percental threshold (50% of local SUV_{max}). Neural networks were trained to segment organs in PET-CT acquisitions (training CTs: 8,632, validation CTs: 53). Thereby, PSMA foci within organs of physiologic PSMA uptake were semi-automatically excluded from the analysis.

Pretherapeutic PSMA-PET-CTs of 40 consecutive patients treated with ^{177}Lu -PSMA-617 therapy were evaluated in this analysis. The volumetric whole-body tumor volume ($PSMA_{TV50}$), SUV_{max} , SUV_{mean} and other whole-body imaging biomarkers were calculated for each patient. Semi-automatically derived results were compared with manual readings in a sub-cohort (by one nuclear medicine physician using *syngo*.MM Oncology software, Siemens Healthineers, Knoxville, TN). Additionally, an inter-observer evaluation of the semi-automated approach was performed in a sub-cohort (by two nuclear medicine physicians).

Results

Manually and semi automatically derived PSMA metrics were highly correlated (PSMA_{TV50}: R²=1.000; p<0.001; SUV_{max}: R²=0.988; p<0.001). The inter-observer agreement of the semi-automated workflow was also high (PSMA_{TV50}: R²=1.000; p<0.001; ICC=1.000; SUV_{max}: R²=0.988; p<0.001; ICC=0.997). PSMA_{TV50} [ml] was a significant predictor of overall survival (HR: 1.004; 95%CI: 1.001-1.006, p=0.002) and remained so in a multivariate regression including other biomarkers (HR: 1.004; 95%CI: 1.001-1.006 p=0.004).

Conclusion

PSMA_{TV50} is a promising PSMA-PET biomarker that is reproducible and easily quantified by the proposed semi-automated software. Moreover, PSMA_{TV50} is a significant predictor of overall survival in patients with advanced prostate cancer that receive ¹⁷⁷Lu-PSMA-617 therapy.

Introduction

Prostate cancer is the most frequent cause of cancer related death in men (1). The precise detection of prostate cancer metastases is of great importance for therapy monitoring and treatment intensification (2). Moreover, metastases are often responsible for prostate cancer related morbidity and mortality (3,4). Thus, the quantification of the whole-body tumor volume is clinically relevant, and we conjecture that it could ultimately predict overall survival (OS) of patients.

Prostate-specific membrane antigen (PSMA) targeting positron emission tomography (PET) has emerged to become the reference standard examination for the diagnostic work up of patients with prostate cancer (5,6). PSMA is a cell surface marker of prostate cancers cells and it is targeted by various ligands both for diagnostic and therapeutic approaches (7,8). However, despite their name, PSMA ligands like PSMA-11 show strong accumulation without pathological implications in many organs like liver, kidneys, salivary glands and others (9,10). Therefore, physiological PSMA accumulations have to be discarded when quantifying image biomarkers.

Image biomarkers have been proposed for various molecular imaging modalities like scintigraphy or PET (11,12). For example, the bone scan index can be quantified automatically using skeletal scintigraphy and has proven to predict the survival of patients with prostate cancer (13). However, skeletal scintigraphy neglects soft tissue metastases, which are of great clinical importance. Yet, only manual or rudimentary automated approaches have been proposed for quantifying the whole-body tumor volume in PSMA-PET-CTs (14,15). While several studies could demonstrate that the change of PSMA-PET-CT derived tumor volume correlates with therapy response, the predictive potential is still poorly elucidated (14,16–19). Importantly, there is no clear evidence that PSMA-PET derived biomarkers can predict the survival of patients with prostate cancer. Finally, most software tools for the automated quantification of PSMA-PET biomarkers utilize a global SUV

threshold for the segmentation of prostate cancer foci (14,15). This procedure may neglect partial volume effects that hamper a sound tumor volume quantification (20–22). Additionally, global thresholding violates the EANM recommendation for molecular volume quantification, which suggests percental thresholding (e.g. 50% of maximal lesion SUV should be used for segmentation of the very same lesion) (23).

In this manuscript, we propose and evaluate a novel semi-automated software, which quantifies the whole-body tumor volume in PSMA-PET-CT. Percental thresholding is used in analogy to EANM guidelines for FDG. Moreover, a neural network is employed, which semi-automatically excludes many physiological PSMA foci from the quantification. Finally, we estimate the survival of patients with advanced prostate cancer who are receiving systemic therapy.

Methods

Patients

To enable the automated organ segmentation, a total number of 8,685 CT scans were labeled by a team of experienced annotators mentored and reviewed by a radiologist. Data was rigorously split for training (n = 8,632) and validation (n = 53 CTs) of the neural networks dedicated to organ segmentation. All data involved in organ segmentation development were independent from the PSMA-PET-CTs.

For the analysis of PSMA-PET-CT biomarkers, a total number of 40 consecutive patients suffering from metastasized castration resistant prostate cancer were included in this study. Patients were treated with ^{177}Lu -PSMA-617 therapy in the department of nuclear medicine in Münster from 12/2014 to 12/2016. PSMA-PET-CTs were acquired before start of therapy. Overall survival (OS) time until death or censoring was recorded. Blood parameters were obtained immediately before the admission of the first therapy administration. Detailed patient characteristics are summarized in Table 1. The retrospective analysis was approved by the local ethics committee (No. 2016-585-f-S, Ethikkommission der Ärztekammer Westfalen-Lippe und der Westfälischen Wilhelms-Universität Münster).

PET acquisition

A Biograph mCT (Siemens Healthineers, Knoxville, TN, United States) was used for PET-CT acquisitions. The PSMA-11 precursor was provided by ABX (ABX GmbH, Radeberg, Germany). A GalliaPharm Gallium generator was used (Eckert & Ziegler, Berlin, Germany). Intravenous administration of ^{68}Ga -PSMA-11 was body weight dependent (2 MBq/kg body weight). PET-CT image acquisition (vertex to proximal tibia) was started 60 minutes after tracer administration. Image reconstruction was done in analogy to previous publications (11). Patients were asked to

void their bladder before imaging. Either low-dose or contrast enhanced CT acquisitions were acquired directly before PET acquisition.

Semi-automated software

A novel software was developed for the semi-automated analysis of PSMA-PET-CT acquisitions to quantify the whole-body tumor volume in a three-step approach (see Figure 1 for overall workflow). To this end, all pathological PSMA avid foci have to be delimited. This has been implemented in the research prototype software MI Whole Body Analysis Suite (MIWBAS, v1.0, Siemens Medical Solutions USA, Inc., Knoxville, TN).

Step 1: Automated PSMA foci segmentation

A patient specific global threshold ($threshold_{PSMA}$) was defined to select voxel clusters with increased PSMA expression:

$$threshold_{PSMA} = \frac{4.30}{SUV_{mean}} * (SUV_{mean} + SUV_{SD}),$$

where SUV_{mean} and SUV_{SD} denote mean and standard deviation of a spherical liver ROI (15 mm radius). This equation was adopted from the qPSMA approach of Gafita et al. (15). The liver reference ROI, which is needed to obtain SUV_{mean} and SUV_{SD} , was automatically positioned (24). To this end, the center of the right liver lobe was automatically determined. Manual adjustments of ROI positioning were only necessary in case of liver metastases. We utilize this threshold for the entire PET acquisition to select voxel clusters (i.e. for bone foci and soft tissue foci). Manual adjustments were carried out in case of liver metastases. A convolution of the PSMA-PET with a 1 ml sphere was performed to obtain SUV_{peak} , which was only utilized for the selection of voxel clusters in analogy to PERCIST (25).

First, voxels with a SUV_{peak} exceeding the $threshold_{PSMA}$ were selected in the whole body PSMA-PET acquisition to form voxel clusters (i.e. group of adjacent voxels). Small voxel clusters falling below a volume of 0.5 ml were discarded. Second, each voxel cluster is segmented based on the local SUV_{max} of the given cluster, which may enlarge or shrink the cluster size. To this end, all voxels of the cluster exceeding 50% of the local SUV_{max} are regarded as portions of the cluster. This procedure is done iteratively, starting with the voxel cluster with the highest SUV_{max} . Thereby, voxel clusters are successively transformed to candidate foci, which may resemble physiological or pathological PSMA accumulation (Figure 2). The assignment of these foci to anatomical locations is described in step 2, the removal of physiological PSMA uptake in step 3.

Step 2: Automated organ segmentation

The anatomical position of each candidate focus was automatically determined to exclude foci of organs with physiologic tracer uptake and to quantify the tumor volume with respect to certain organs. The following organs were therefore chosen for automated segmentation: liver, kidneys, bladder, heart, lungs, brain and skeleton. The algorithm segmented these organs with a generative adversarial network (GAN) in a three-step inference using CT data: First, a set of 126 anatomical landmarks, including vessel bifurcations, bony structures, and organ center and boundary points, were detected in the CT (26). Preliminary region of interests (ROI) of each individual organ based on the detected landmarks were extracted and fed to a dedicated organ segmentation network for refinement. The preliminary ROIs were substantially smaller than the CT volume, which improved the consistency by focusing on regional variations rather than variations in the overall image and increased efficiency by reducing computational load. For the skeleton, the ROI was the entire CT volume (27). Second, a dedicated Deep Image-to-Image Network (DI2IN) was employed for the final segmentation of each organ (28). It consisted of a convolutional encoder-decoder architecture combined with multi-level feature concatenation. For training, an adversarial network was

selectively used to regularize the training process of DI2IN by discriminating the output of DI2IN from the ground truth in a patch-by-patch manner using binary cross-entropy. For validation, the segmentation quality was measured as Dice Similarity Coefficient (DSC) between the segmentation and the ground truth of the validation set in resampled resolutions, where DSC is a volumetric overlap metric between two mask volumes, e.g., A and B:

$$DSC(A, B) = \frac{2|A \cap B|}{|A| + |B|}$$

Third, each organ segmentation mask was transferred to the PET data.

Step 3: Semi-automated determination of image biomarkers

Candidate foci within organs with physiological PSMA accumulation (liver, spleen, bladder, kidneys) are automatically excluded. Candidate foci within other organs with physiologic PSMA uptake like small bowel, salivary and tear glands, ganglia and others had to be manually discarded. If physiological foci were erroneously missed by the software, they were manually removed. Thereby, only foci with pathological PSMA uptake remain in the analysis (i.e. pathological foci).

Biomarkers were calculated for soft tissue, the skeleton and the whole patient: The volumes of segmented lesions were summed to obtain the whole-body tumor volume ($PSMA_{TV50}$). In analogy to total lesion glycolysis, $PSMA_{TL}$ was quantified as product of $PSMA_{TV50}$ and SUV_{mean} . Additionally, highest SUV_{max} and SUV_{peak} as well as averaged SUV_{mean} were quantified.

Manual PSMA-PET measurements and inter-observer agreement

First, manual reads of PSMA-PET-CTs were done by R.S. (>2 years of clinical PET experience) using *syngo.MM Oncology* software (Siemens Healthineers, Knoxville, TN, United States) to quantify $PSMA_{TV50}$, SUV_{mean} , SUV_{peak} and SUV_{max} (the VOI Isocontour segmentation tool was

used, involving manually identifying a spherical region in which 50% of SUV_{max} was used for segmentation). Second, an inter-observer study was done by R.S. and K.R. (>5 years PET experience) independently using the semi-automated software. A sub-cohort of 20 randomly selected patients was used for both purposes due to logistic reasons.

Additionally, the whole-body tumor volume was quantified without 50% percental thresholding for comparison and denoted $PSMA_{TV}$. To this end, manual segmentation of pathological PSMA foci was done in the subgroup using the global $threshold_{PSMA}$. Refinement of the threshold was only done in case of confluent lesions or other visual saliences (e.g. necrotic tumor parts that were erroneously segmented).

Statistical analysis

SPSS 24 (IBM, NY, USA) was used for paired t-tests, log rank test, Cox regression, inter class correlation coefficient (ICC), Spearman's rho (ρ) or Pearson correlational analysis and plotting. MATLAB R2018b (The MathWorks, MA, USA) and Excel 2010 v14.0 (Microsoft, WA, USA) were used for data management. Values are presented as mean together with the 95% confidence interval (95% CI). Mean absolute agreement ICC was calculated using a 2-way mixed effect model. P values < 0.05 was regarded as statistically significant.

Results

Organ segmentation

The automatic organ segmentation demonstrated a mean DSC value of at least 0.86 for every organ. The skeleton segmentation performs accurately with a mean DSC value over 0.92 (95% CI 0.894–0.944). Details are given by Table 2.

Manual measurement of PSMA biomarkers

Manual and semi-automatically quantified whole-body tumor volume did not significantly differ and showed very high correlation (162.8 vs. 173.3 ml, $p=0.107$; $R^2 = 0.996$, $p<0.001$). The same was true for SUV_{max} (58.0 vs. 53.3, $p=0.229$; $R^2 = 0.790$, $p<0.001$), SUV_{peak} (35.1 vs. 35.6, $p=0.541$; $R^2 = 0.964$, $p<0.001$) and SUV_{mean} (16.1 vs. 15.9, $p=0.779$; $R^2 = 0.943$, $p<0.001$). Statistically significant difference was observed for $PSMA_{TL}$ between manual and semi-automated reads (2422.2 vs. 2649.1, $p=0.031$; $R^2 = 0.990$, $p<0.001$).

PSMA-PET CT reading using the semi-automated software was on average 3.3 times faster than using the manual approach and can be accomplished in approximately 2 minutes (average time per patient: 119.6 vs. 397.3 s, $p = 0.02$, $n=10$).

Inter observer agreement of PSMA biomarkers

Whole-body $PSMA_{TV50}$ was very highly correlated ($R^2=1.000$; $p<0.001$) between Reader 1 and 2 (for soft tissue $PSMA_{TV50}$: $R^2=1.000$; $p<0.001$; for skeletal $PSMA_{TV50}$: $R^2=1.000$; $p < 0.001$). The same was true for SUV_{max} ($R^2=0.988$; $p<0.001$), SUV_{mean} ($R^2=0.953$; $p<0.001$) and $PSMA_{LA}$ ($R^2=0.998$; $p<0.001$). ICCs of $PSMA_{TV50}$, $PSMA_{TL}$, SUV_{max} and SUV_{mean} were 1.000 (95%CI: 1.000-1.000), 1.000 (95%CI: 0.999-1.000), 0.997 (95%CI: 0.991-0.999) and 0.988 (95%CI: 0.969-0.995). See Figure 3 for details.

PSMA biomarkers and overall survival

In a first approach, univariate Cox regression was performed for PSMA biomarkers and blood tumor markers. Significant predictors of OS were PSMA_{TV50} (HR: 1.004; p=0.002), and alkaline phosphatase (HR: 1.001; p=0.047). PSMA_{TV50} measured in deciliter had a HR of 1.45. In a second approach, significant predictors were included in a multivariate analysis, in which only PSMA_{TV50} remained significant predictors of OS (HR: 1.004; p=0.004; 95%CI: 1.001-1.006). Detailed results of uni- and multivariate Cox regressions are presented in Table 3 and Figure 4.

Median OS according to PSMA_{TV50} quartiles were (in descending order of tumor volume): 5.3, 7.9, 11.4 and 21.3 months. There was no significant difference comparing OS of patients with regard to the PSMA_{TV50} median (21.3 vs. 6.7 months, p = 0.058). However, OS was significantly longer in quartile 1 of PSMA_{TV50} compared to quartile 4 (21.3 vs. 5.3 months, p < 0.031).

PSMA_{TV50} vs. PSMA_{TV}

Tumor volume measured as PSMA_{TV} was significantly greater compared to PSMA_{TV50} (661.0 vs. 213.0 ml, p < 0.001). However, there was a correlation between PSMA_{TV} and PSMA_{TV50} (R²=0.473; p < 0.001). PSMA_{TV} could not significantly predict OS (HR: 1.001; p=0.062; 95%CI: 1.000-1.001) in univariate Cox-regression. Likewise, there was no significant difference regarding OS between quartile 4 and quartile 1 of PSMA_{TV} (7 vs. 7.5 months, p = 0.235).

PSMA biomarkers and blood parameters

There were moderate correlations between whole-body PSMA_{TV50} and blood levels of prostate specific antigen (ρ =0.553; p<0.001) or skeletal PSMA_{TV50} and alkaline phosphatase (ρ =0.525; p=0.001; see Figure 5).

Discussion

The semi-automated quantification of PSMA-PET biomarkers like the whole-body tumor volume by the proposed software was significantly faster compared to manual PET-CT readings and can be achieved on average in 2 minutes, and the correlation between manual and semi-automated reading was excellent. In contrast to previously proposed approaches, percental thresholding was employed and no time-consuming refinement of image segmentation masks is needed. Moreover, the semi-automatically quantified tumor volume ($PSMA_{TV50}$) could significantly predict OS of patients with advanced prostate cancer.

Imaging derived biomarkers, like whole-body tumor volume, are excellent predictors of survival in patients with various metastasized diseases (29,30). For prostate cancer, the quantification of the fraction of metastatically affected bones in planar bone scintigraphy could accurately stratify patients according to symptomatic progression and overall survival in a prospective phase III trial (30). Several approaches have been proposed to (semi)-automatically quantify tumor volumes in PSMA-PET-CT (11,14,15,31). It was shown previously, that the change of whole-body tumor volume correlated with the overall response (14,16). Yet, the relevance of PSMA-PET imaging biomarkers as predictors of survival in patients with prostate cancer is poorly elucidated. The present work could demonstrate that $PSMA_{TV50}$ is a significant predictor of survival in patients with advanced prostate cancer that undergo ^{177}Lu -PSMA-617 therapy. An increase of 100 ml in whole body tumor volume ($PSMA_{TV50}$) is associated with a 1.4-fold higher risk of death. Interestingly, $PSMA_{TL}$ did not significantly predict overall survival. This strengthens the assumption, that PSMA-SUV does not predict response to systemic therapy, which clarifies the need of novel PET biomarkers like $PSMA_{TV50}$.

Organs of physiologic PSMA ligand excretion have to be excluded when quantifying whole-body tumor volume or other biomarkers. To this end, various approaches have been proposed to assist the reader in removing physiologic accumulations (14,15). A generative adversarial network (GAN) is employed by the proposed software for automated organ segmentation. The CT component is used by the neural network to extract anatomical landmarks and segmentations, which are transferred to the PET component by rigid transformation. The Dice Similarity Coefficient, which is measuring the accuracy segmentation, is higher for the proposed software (mean: 0.926) compared to the software qPSMA (77.4 - 85.6) when analyzing the skeleton mask (18).

In contrast to other semi-automated software packages, the proposed software uses percental thresholding of PSMA foci: For each focus, 50% of the maximal SUV is automatically used for confinement. This is in line with EANM guidelines for FDG-PET, which recommend percental thresholding by using 41% or 50% of the maximum SUV for volumetric analyses (23). The utilization of percental thresholding is advantageous both in technical and physical regard:

The technical (i) advantage of percental thresholding is that adjacent metastases are separated and the whole-body tumor burden is dismembered in separate lesions. Thereby, each focus can automatically be assigned to an anatomical location. Foci assigned to organs with known physiological excretion can thus be rule based removed (e.g. kidney, ureter, etc.). Moreover, the user is not requested to exclude missed physiological foci by the manual adjustment of masks, but rather by deletion of the individual focus. Thus, the need of user interaction is reduced to a minimum level. This is in contrast to global thresholding, which results in large confluent ROIs combining physiological and pathological foci (15). The physical (ii) benefit of percental thresholding is that the lesion size can be quantified accurately. In contrast, segmenting lesions by

a global threshold is prone to overestimating the volume. This is because of positron range and partial volume effects, which induces image blur (22). Therefore, percental thresholding is a prerequisite for correct volumetric analyses.

Despite the twofold advantage of percental thresholding, there was a high correlation between whole-body tumor volume between $PSMA_{TV}$ and $PSMA_{TV50}$. However, $PSMA_{TV50}$ was significantly smaller compared to $PSMA_{TV}$. Interestingly, $PSMA_{TV}$ could not significantly predict OS, indicating that percental thresholding should be implemented in modern assisted reading software.

The present study faces some limitations. Only a relatively small number of patients were included, which may hamper the generalizability to a larger population. Additionally, all enrolled patients received Lu-PSMA therapy after the quantification of PSMA biomarkers. Lu-PSMA therapy is targeting the same molecule that is visualized by PSMA-PET. The survival prediction might therefore be biased. Moreover, one could argue that a decrease of the local SUV_{max} in response to therapy, would cause $PSMA_{TV50}$ to paradoxically increase. However, solitary changes only of SUV_{max} seem unrealistic. Rather, not only SUV_{max} , but the uptake of the entire lesion should concordantly decrease in response to therapy in this scenario. Therefore, $PSMA_{TV50}$ would decrease and thus correctly assess therapy response. Yet, future studies should evaluate $PSMA_{TV50}$ as biomarker for therapy response.

The physiological uptake of PSMA tracer varies, especially ^{18}F -PSMA-1007 has a fundamentally different physiological uptake due to liver dominant excretion (32). The liver reference ROI might be unsuitable to provide a patient specific $threshold_{PSMA}$ for foci selection in ^{18}F -PSMA-1007 PET-CT acquisitions. Therefore, future studies should evaluate blood pool activity as reference for ligand agnostic definitions of $threshold_{PSMA}$.

The metastatic extent of the cohort was heterogenous and confidence intervals of regression were relatively large. Additionally, liver metastasis with small tumor volume might still have heavily influenced overall survival. This could have distorted the relationship of tumor volume to overall survival. Future studies should evaluate the predictive potential of PSMA_{TV50} in larger homogeneous patient cohorts that receive anti-cancer therapies distinct from Lu-PSMA.

Conclusion

The quantification of PSMA-PET-CT biomarkers using the proposed software is feasible and achieves excellent inter-observer agreement. Semi-automated PET reading is faster than manual analysis. Moreover, semi-automatically derived PSMA_{TV50} biomarker is a significant predictor of OS in patients with advanced prostate cancer, whereas PSMA_{TV} is not. Future studies elucidating the predictive potential of PSMA_{TV50} seem warranted.

Disclosure statement

KR received consultant fees from ABX and Bayer Healthcare and lectureship fees from AAA, SIRTEX, AMGEN and Janssen Cielag. VS, ZX, GC, SG and BS are full time employees of Siemens Medical Solutions, USA, Inc.

KEY POINTS

QUESTION: Can PSMA-PET based tumor volume be quantified by a semi-automated software and be used as a prognostic biomarker of overall survival?

PERTINENT FINDINGS: Semi-automated PET reading is feasible, has high inter observer agreement and is faster than manual analysis. Semi automatically derived tumor volume is a significant predictor of overall survival time whereas blood tumor markers are not.

IMPLICATIONS FOR PATIENT CARE: Semi-automatically derived tumor volume is a significant predictor of overall survival time in patients with advanced prostate cancer.

References

1. Siegel RL, Miller KD, Jemal A. Cancer Statistics, 2017. *CA Cancer J Clin.* 2017;67:7-30.
2. Sartor O, de Bono JS. Metastatic Prostate Cancer. Longo DL, ed. *N Engl J Med.* 2018;378:645-657.
3. Halabi S, Kelly WK, Ma H, et al. Meta-analysis evaluating the impact of site of metastasis on overall survival in men with castration-resistant prostate cancer. *J Clin Oncol.* 2016;34:1652-1659.
4. DePuy V, Anstrom KJ, Castel LD, Schulman KA, Weinfurt KP, Saad F. Effects of skeletal morbidities on longitudinal patient-reported outcomes and survival in patients with metastatic prostate cancer. *Support Care Cancer.* 2007;15:869-876.
5. Fendler WP, Calais J, Eiber M, et al. Assessment of 68Ga-PSMA-11 PET Accuracy in Localizing Recurrent Prostate Cancer: A Prospective Single-Arm Clinical Trial. *JAMA Oncol.* 2019;5:856-863.
6. Fendler WP, Weber M, Irvani A, et al. Prostate-Specific Membrane Antigen Ligand Positron-Emission Tomography in Men with Nonmetastatic Castration-Resistant Prostate Cancer. *Clin Cancer Res.* 2019:clincanres.1050.2019.
7. Afshar-Oromieh A, Babich JW, Kratochwil C, et al. The Rise of PSMA Ligands for Diagnosis and Therapy of Prostate Cancer. *J Nucl Med.* 2016;57:79S-89S.
8. Rahbar K, Afshar-Oromieh A, Jadvar H, Ahmadzadehfar H. PSMA Theranostics: Current Status and Future Directions. *Mol Imaging.* 2018;17:1536012118776068.
9. Hofman MS, Hicks RJ, Maurer T, Eiber M. Prostate-specific membrane antigen PET: Clinical utility in prostate cancer, normal patterns, pearls, and pitfalls. *Radiographics.* 2018;38:200-217.
10. Backhaus P, Noto B, Avramovic N, et al. Targeting PSMA by radioligands in non-prostate

- disease—current status and future perspectives. *Eur J Nucl Med Mol Imaging*. 2018;45:860-877.
11. Bieth M, Krönke M, Tauber R, et al. Exploring New Multimodal Quantitative Imaging Indices for the Assessment of Osseous Tumor Burden in Prostate Cancer Using 68Ga-PSMA PET/CT. *J Nucl Med*. 2017;58:1632-1637.
 12. Nakajima K, Edenbrandt L, Mizokami A. Bone scan index: A new biomarker of bone metastasis in patients with prostate cancer. *Int J Urol*. 2017;24:668-673.
 13. Smith M, De Bono J, Sternberg C, et al. Phase III Study of Cabozantinib in Previously Treated Metastatic Castration-Resistant Prostate Cancer: COMET-1. *J Clin Oncol*. 2016;34:3005-3013.
 14. Grubmüller B, Senn D, Kramer G, et al. Response assessment using 68 Ga-PSMA ligand PET in patients undergoing 177 Lu-PSMA radioligand therapy for metastatic castration-resistant prostate cancer. *Eur J Nucl Med Mol Imaging*. 2019;46:1063-1072.
 15. Gafita A, Bieth M, Krönke M, et al. qPSMA: Semiautomatic Software for Whole-Body Tumor Burden Assessment in Prostate Cancer Using 68 Ga-PSMA11 PET/CT . *J Nucl Med*. 2019;60:1277-1283.
 16. Grubmüller B, Rasul S, Baltzer P, et al. Response assessment using [68 Ga]Ga-PSMA ligand PET in patients undergoing systemic therapy for metastatic castration-resistant prostate cancer. *Prostate*. October 2019;pros.23919.
 17. Schmidkonz C, Cordes M, Schmidt D, et al. 68Ga-PSMA-11 PET/CT-derived metabolic parameters for determination of whole-body tumor burden and treatment response in prostate cancer. *Eur J Nucl Med Mol Imaging*. 2018;45:1862-1872.
 18. Bieth M, Peter L, Nekolla SG, et al. Segmentation of Skeleton and Organs in Whole-Body CT Images via Iterative Trilateration. *IEEE Trans Med Imaging*. 2017;36:2276-2286.

19. Schmuck S, Von Klot CA, Henkenberens C, et al. Initial experience with volumetric ⁶⁸Ga-PSMA I&T PET/CT for assessment of whole-body tumor burden as a quantitative imaging biomarker in patients with prostate cancer. *J Nucl Med.* 2017;58:1962-1968.
20. Jentzen W, Freudenberg L, Eising EG, Heinze M, Brandau W, Bockisch A. Segmentation of PET volumes by iterative image thresholding. *J Nucl Med.* 2007;48:108-114.
21. Soret M, Bacharach SL, Buvat I. Partial-volume effect in PET tumor imaging. *J Nucl Med.* 2007;48:932-945.
22. Erdi YE, Mawlawi O, Larson SM, et al. Segmentation of lung lesion volume by adaptive positron emission tomography image thresholding. *Cancer.* 1997;80:2505-2509.
23. Boellaard R, Delgado-Bolton R, Oyen WJG, et al. FDG PET/CT: EANM procedure guidelines for tumour imaging: version 2.0. *Eur J Nucl Med Mol Imaging.* 2015;42:328-354.
24. Tao Y, Peng Z, Krishnan A, Zhou XS. Robust learning-based parsing and annotation of medical radiographs. *IEEE Trans Med Imaging.* 2011;30:338-350.
25. Wahl RL, Jacene H, Kasamon Y, Lodge MA. From RECIST to PERCIST: Evolving considerations for PET response criteria in solid tumors. *J Nucl Med.* 2009;50:122-151.
26. Ghesu FC, Georgescu B, Zheng Y, et al. Multi-Scale Deep Reinforcement Learning for Real-Time 3D-Landmark Detection in CT Scans. *IEEE Trans Pattern Anal Mach Intell.* 2019;41:176-189.
27. Lindgren Belal S, Sadik M, Kaboteh R, et al. Deep learning for segmentation of 49 selected bones in CT scans: First step in automated PET/CT-based 3D quantification of skeletal metastases. *Eur J Radiol.* 2019;113:89-95.
28. Yang D, Xu D, Zhou SK, et al. Automatic Liver Segmentation Using an Adversarial Image-to-Image Network. In: Lecture Notes in Computer Science (Including Subseries Lecture Notes in Artificial Intelligence and Lecture Notes in Bioinformatics). Vol 10435 LNCS. ;

2017:507-515.

29. Chen S, He K, Feng F, et al. Metabolic tumor burden on baseline 18F-FDG PET/CT improves risk stratification in pediatric patients with mature B-cell lymphoma. *Eur J Nucl Med Mol Imaging*. 2019;46:1830-1839.
30. Armstrong AJ, Anand A, Edenbrandt L, et al. Phase 3 assessment of the automated bone scan index as a prognostic imaging biomarker of overall survival in men with metastatic castration-resistant prostate cancer a secondary analysis of a randomized clinical trial. *JAMA Oncol*. 2018;4:944-951.
31. Hammes J, Täger P, Drzezga A. EBONI: A tool for automated quantification of bone metastasis load in PSMA PET/CT. *J Nucl Med*. 2017:jnumed.117.203265-24.
32. Eiber M, Herrmann K, Calais J, et al. Prostate cancer molecular imaging standardized evaluation (PROMISE): Proposed miTNM classification for the interpretation of PSMA-ligand PET/CT. *J Nucl Med*. 2018;59:469-478.

Figures

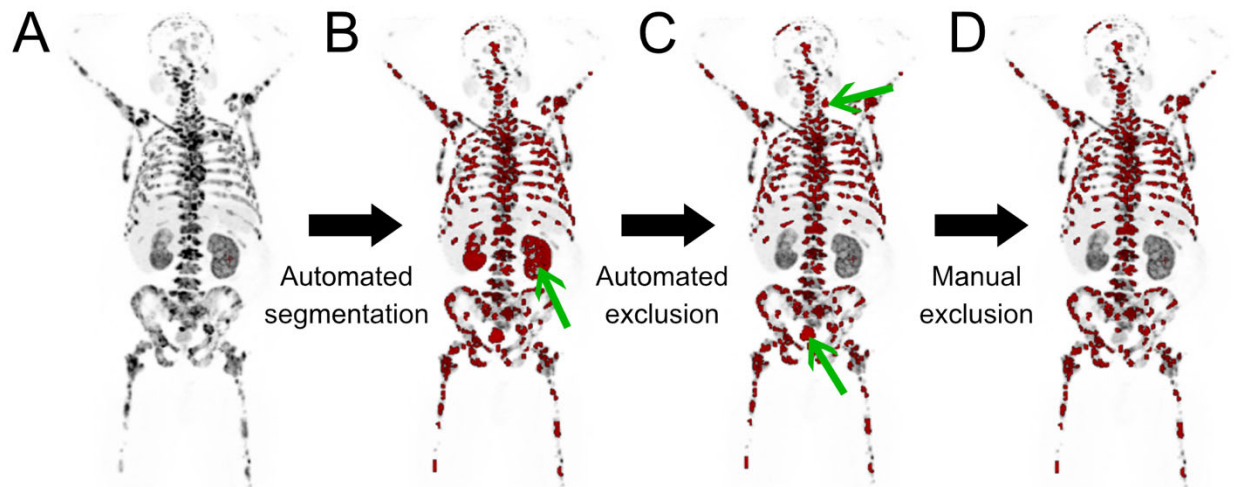


Figure 1: Overall workflow

Maximum Intensity Projection (MIP) of a ^{68}Ga -PSMA-11 PET (A-D). Automatically selected and segmented foci are overlaid in red. The proposed software first segments all PSMA foci (step 1; A), delineates the organs of physiological tracer uptake (step 2; B) and finally semi automatically excludes PSMA foci within these organs (step 3; C, D). The automated exclusion of physiologic organs removed the kidneys (exemplary green arrow in B). However, the bladder and a salivary gland were missed and thus manually excluded from the analysis (green arrow in C). The final segmentation is shown by panel D.

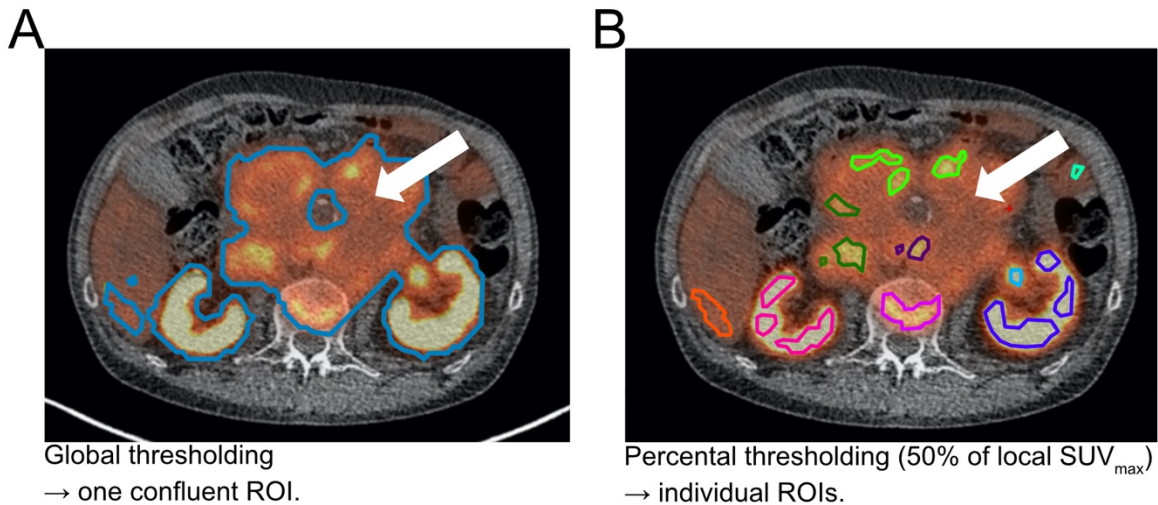


Figure 2: Segmentation concepts.

^{68}Ga -PSMA-11 PET-CT of a patient with partly necrotic and thus low PSMA accumulating lymph node metastases (arrows). Segmentation of PSMA foci is done by a fixed global threshold alone (A) or by the consecutive application of the same global threshold followed by a local percental threshold (50% of SUV_{max}) for each focus (B). Global thresholding is erroneously selecting necrotic tumor parts as well as vital metastases. Moreover, global thresholding is producing a large confluent ROI, which includes both kidneys, a bone metastasis and parts of the liver (A). Corrections would require voxel-wise manipulations. In contrast, the additional application of percental thresholds (50% of SUV_{max}) result in multiple ROIs (indicated by separate colors), which are not confluent and exclude necrotic tumor parts (B). Moreover, physiologic uptake can easily be discarded by semi-automated deletion of ROIs in organs with physiologic uptake.

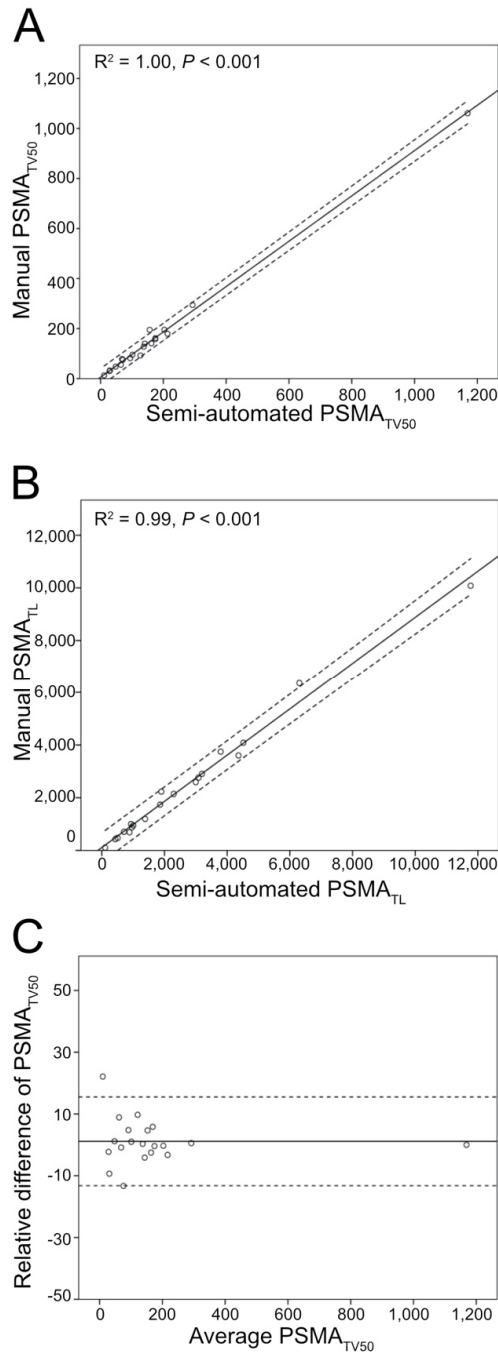


Figure 3: Evaluation of the proposed software.

The semi-automatically derived whole-body PSMA_{TV50} is very highly correlated with the volume of all manually segmented lesions (A). The same is true for the whole-body SUV_{max} (B). A Bland-Altman plot of the inter-observer agreement is shown in panel C. A subcohort ($n = 20$) was used for these analyses.

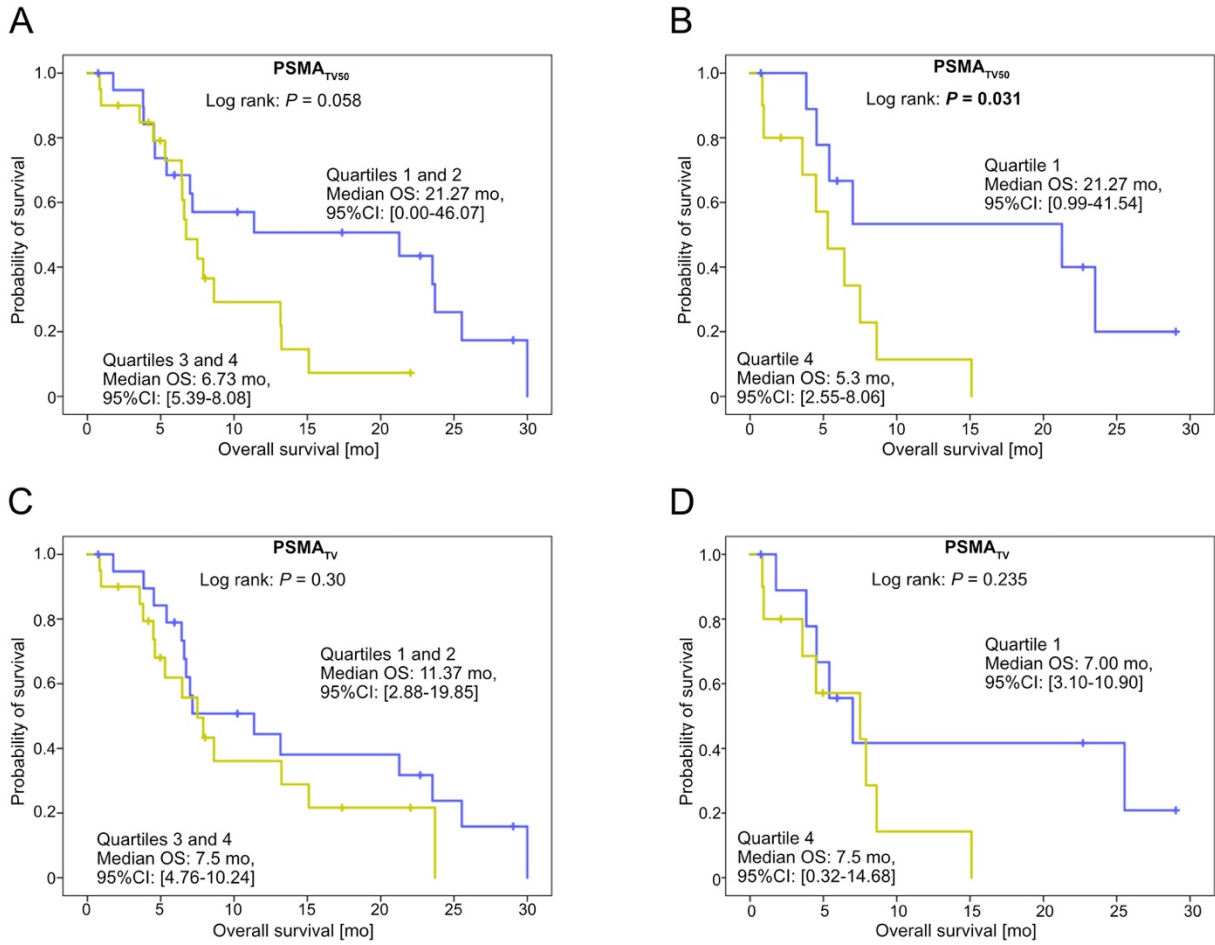


Figure 4: Overall survival stratified by the whole-body tumor volume, which was measured by the proposed software.

All patients ($n = 40$) were stratified by whole-body PSMA_{TV50} quartiles (A and B) or PSMA_{TV} quartiles (C and D).

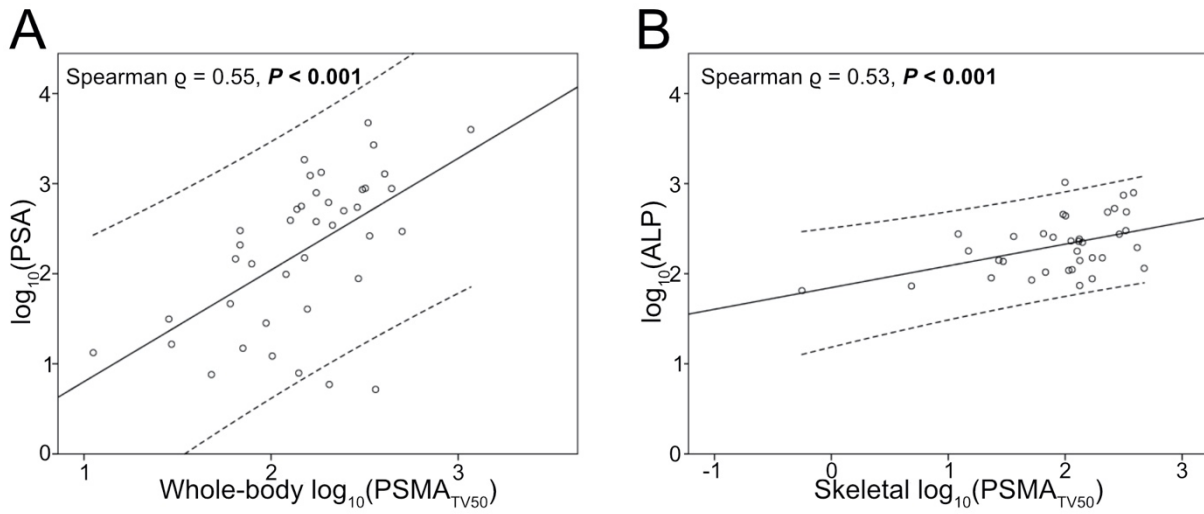


Figure 5: Correlation of imaging and blood biomarkers.

There was a moderate correlation between whole-body PSMA_{TV} and prostate specific antigen (PSA) levels (A). The same was true for skeletal PSMA_{TV} and alkaline phosphatase levels (B).

Values were plotted after \log_{10} transformation.

Tables

Table 1: patient characteristics.

<i>Patient characteristics</i>	Mean [SD]	N [%]
Total number of patients		40 [100]
Age	73.7 [5.9]	
PSA levels [ng/ml]	656.7 [1034.3]	
ALP levels [U/l]	250.1 [219.2]	
History of Docetaxel chemotherapy		27 [67.5]
History of Cabazitaxel chemotherapy		9 [22.5]
Site of metastases		
• Liver metastases		14 [35.0]
• Bone metastases		37 [92.5]
• Lymph node metastases		36 [90.0]
• Lung metastases		13 [32.5]

PSA: prostate specific membrane antigen; ALP: alkaline phosphatase; SD: standard deviation.

Table 2: Numbers of training and validation data for each organ and the Dice Similarity Coefficient (DSC) over the validation set.

Organ	N of training CTs	N of validation CTs	DSC Mean [95% CI]
Brain	200	11	0.973 [0.959-0.981]
Heart	386	32	0.865 [0.725-0.927]
Liver	1788	31	0.965 [0.937-0.978]
Kidney Left	1508	32	0.932 [0.759-0.967]
Kidney Right	1750	32	0.942 [0.841-0.968]
Lungs	5000	32	0.958 [0.915-0.973]
Bladder	724	20	0.930 [0.647-0.980]
Skeleton	768	33	0.926 [0.894–0.944]

Training and validation sets varied across different organs due to the availability of manual annotations from clinical experts.

Table 3: Cox regressions of survival and biomarkers.

Cox Regression	Covariates	HR	95% CI	P value
Univariate	whole-body PSMA _{TV50}	1.004	1.001-1.006	0.002
	whole-body PSMA _{LA}	1.000	1.000-1.000	0.077
	whole-body SUV _{max}	0.997	0.985-1.008	0.583
	whole-body SUV _{peak}	0.995	0.976-1.013	0.573
	whole-body SUV _{mean}	0.977	0.924-1.033	0.411
	ALP	1.001	1.000-1.003	0.047
	PSA	1.000	1.000-1.001	0.066
Multivariate	whole-body PSMA _{TV50}	1.004	1.001-1.006	0.004
	ALP	1.001	1.000-1.003	0.115

PSMA_{TV}: volume of PSMA positive tumor [ml]; PSMA_{LA}: volume of PSMA positive tumor multiplied by SUV_{mean}; PSA: prostate specific antigen; ALP: alkaline phosphatase; HR: hazard ratio; CI: confidence Interval.